Paleomagnetism indicates no Neogene rotation of the Qaidam Basin in northern Tibet during Indo-Asian collision

Guillaume Dupont-Nivet, Robert F. Butler — Department of Geosciences, University of Arizona, Tucson, Arizona 85721, USA
An Yin — Department of Earth and Space Sciences, University of California, Los Angeles, California 90095, USA
Xuanhua Chen — Institute of Geomechanics, Beijing, 10081, People's Republic of China

ABSTRACT

Paleomagnetic data were obtained from Tertiary red sedimentary rocks at two locations separated by several hundred kilometers within the Qaidam Basin. In the east-central part of the basin, 30 sites from the lower Pliocene Youshashan Formation yielded characteristic remanent magnetization (ChRM) directions with intermediate unblocking temperatures (100–600 °C); ChRM with high unblocking temperatures (to 680 °C) was isolated from 14 sites. In the same area, ChRM directions were obtained from six sites within the Oligocene Lower Gancaigou Formation. Characteristic magnetization was also determined from 16 sites within the Lower Gancaigou Formation exposed in the E Bo Liang range of the north-central Qaidam Basin. When compared with equivalent-age expected directions for Eurasia, the mean paleomagnetic directions indicate no Neogene vertical-axis rotation of the Qaidam Basin or the Altyn Tagh fault. The Qaidam Basin may act as an indentor translating without rotation toward the North China block and driving clockwise vertical-axis rotations by differential shortening within the Nan Shan fold-and-thrust belt.

Keywords: paleomagnetism, tectonic rotations, Qaidam Basin, eastern Tibet.

INTRODUCTION

Evaluation of geodynamic models for the Himalaya-Tibetan orogen (England and Houseman, 1986; Royden et al., 1997; Tapponnier et al., 1982) requires knowledge of the kinematics in this collisional mountain system, including vertical-axis rotations of crustal blocks and bounding faults. Geodetic and seismic analyses provide kinematic detail over years to decades (Bendick et al., 2000; Chen et al., 2000; Holt and Haines, 1993). Geomorphic and Quaternary slip-rate observations provide kinematic estimates over time scales approaching 10^6 yr (Meyer et al., 1998). Some of these analyses have indicated clockwise vertical-axis rotation of large parts of the northeast Tibetan Plateau, including the Qaidam Basin, at rates of 1°–2°/m.y. (Peltzer and Saucier, 1996). Paleomagnetism can determine net vertical-axis rotation of crustal blocks over 10^6–10^9 yr (Beck et al., 1986; Chen et al., 1993a; Gilder et al., 1996). Here we report paleomagnetic data from the interior of the Qaidam Basin that limit rotation to $\leq$5° over the past 30 m.y.

The Qaidam Basin (Fig. 1) is a relatively low elevation region of 1.2×10^5 km^2 in the northeast Tibetan Plateau bounded by the Altyn Tagh fault to the northwest, the Kunlun fault to the south, and the Nan Shan fold-and-thrust belt to the northeast. Compared to complexly deformed surrounding areas, the Qaidam Basin shows only limited deformation of the Cretaceous to Tertiary sedimentary cover (Meyer et al., 1998). This change in elevation and intensity of deformation is attributed to higher strength of the Qaidam crust (Zhu et al., 1995) compared to surrounding regions that underwent compressional deformation and attendant crustal thickening. Although these characteristics make the Qaidam Basin an important target for studying vertical-axis rotations related to the Himalaya-Tibetan orogen, outcrop areas within the basin are limited and often difficult to access. We obtained paleomagnetic samples from two areas of exposed Tertiary red sedimentary rocks (Fig. 1) and present the results in this paper.

METHODS

Eight oriented core samples were collected at each site (sedimentary horizon). After initial measurement of natural remanent magnetization (NRM), samples were thermally demagnetized at 10–20 temperatures from 50 to 700 °C. Typical demagnetization behaviors are illustrated in Figure DR1[1]. Whereas some samples yielded erratic demagnetization behavior from which characteristic remanent magnetization (ChRM) directions could not be determined (Fig. DR1, A), the majority of samples revealed a ChRM at unblocking temperatures >400 °C (Fig. DR1, B, C, and D).

Results from four or more successive temperatures were analyzed by principal component analysis (Kirschvink, 1980) to determine sample ChRM directions. The maximum angular deviation (MAD) for samples yielding ChRM directions was generally <5°; samples yielding MAD >15° were rejected for further analysis. Site-mean ChRM directions were calculated by using methods of Fisher (1953). When one sample ChRM direction from a site was divergent from the preliminary site-mean direction by more than two angular standard deviations, that direction was rejected prior to final calculation of site-mean direction. All site-mean directions from sites with four or more sample ChRM directions are listed in Table DR1 (see footnote 1) and were used to calculate section-mean directions.

XIAO QAIDAM RESULTS

Southwest of Xiao Qaidam, paleomagnetic samples were collected across a broad anticline in two stratigraphic sections (Fig. 2A). The Xiao Qaidam section A (XQA section) is composed of 22 sites in dark red sandstones covering ~200 m of folded strata in the Oligocene Lower Gancaigou Formation (Qinghai Bureau of Geology and Mineral Resources, 1991). Only seven sites provided well-determined site-mean characteristic magnetization directions (Fig. 2B) because the coarser sandstones produced erratic thermal-demagnetization behavior (Fig. DR1, A). Concentration of unblocking temperatures in the 650–685 °C range for the characteristic component (Fig. DR1, B) and rock-magnetic experiments indicate that this magnetization is carried by hematite. One site-mean direction was discarded on the basis of its aberrant direction that probably resulted from local structural complexity in this folded section. The remaining site-mean directions pass a fold test (McFadden, 1990) at 99% confidence; the single normal-polarity site-mean direction is indistinguishable from the antipode of the mean computed from the reverse-polarity sites. These observations suggest a primary origin for the stable paleomagnetism in the XQA section. When compared to the expected Eurasian Oligocene declination (Besse and Courtillot, 1991) at the sampling location, the section-mean declination indicates no significant vertical-axis rotation since the Oligocene (Fig. 2B; Table 1). As explained subsequently, we interpret the flattening of inclination to be a depositional or compaction effect without tectonic significance.

[1]GSA Data Repository item 2002023, Table 1, Site-mean paleomagnetic directions, Table 2, Paleomagnetic results from eastern Tibetan Plateau, and Figure DR1, Vector-component diagrams of thermal-demagnetization behavior, is available on request from Documents Secretary, GSA, P.O. Box 9140, Boulder, CO 80301-9140, editing@geosociety.org, or at www.geosociety.org/pubs/ft2002.htm.

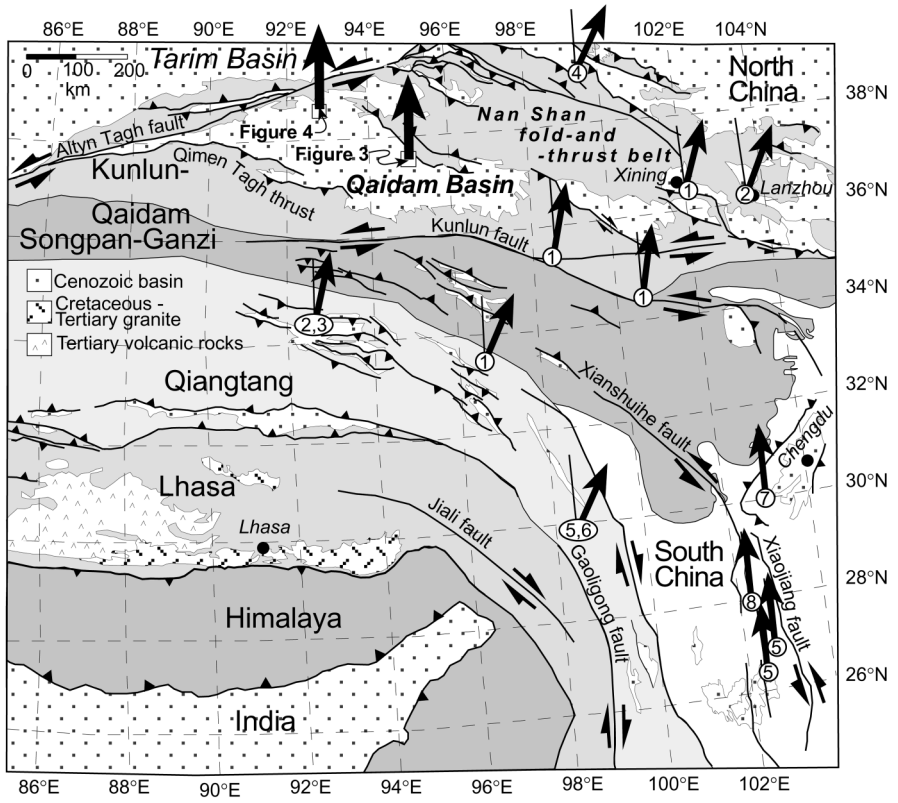

Figure 1. Terranes, basins, and major faults of eastern Tibetan Plateau and adjacent regions (Yin and Harrison, 2000). Large arrows illustrate paleomagnetic declinations from wihair Qaidam Basin (this study). Smaller arrows illustrate paleomagnetic declinations from other areas compared to expected declinations indicated by line. Numbers indicate references listed in Table DR2 (see footnote 1).

The Xiao Qaidam section B (XQB section) covers a stratigraphic thickness >150 m along a 17 km subcrop of light brown muddy sandstones in the lower Pliocene Youshashan Formation (Qinghai Bureau of Geology and Mineral Resources, 1991) (Fig. 2A). The construction of a petroleum pipeline during our field sampling permitted collection of paleomagnetic samples from 33 stratigraphic levels in the walls of the pipeline ditch. Following removal of a present-field component by thermal demagnetization to 100 °C, two stable paleomagnetic components were observed (Fig. DR1, C): (1) an intermediate-temperature component (ITC) with unblocking temperatures in the 100–600 °C range, probably carried by magnetite, and (2) a high-temperature component (HTC) with unblocking temperatures dominantly in the 660–685 °C range, suggesting a hematite carrier. Aside from three sites with samples showing erratic demagnetization behavior, site-mean directions

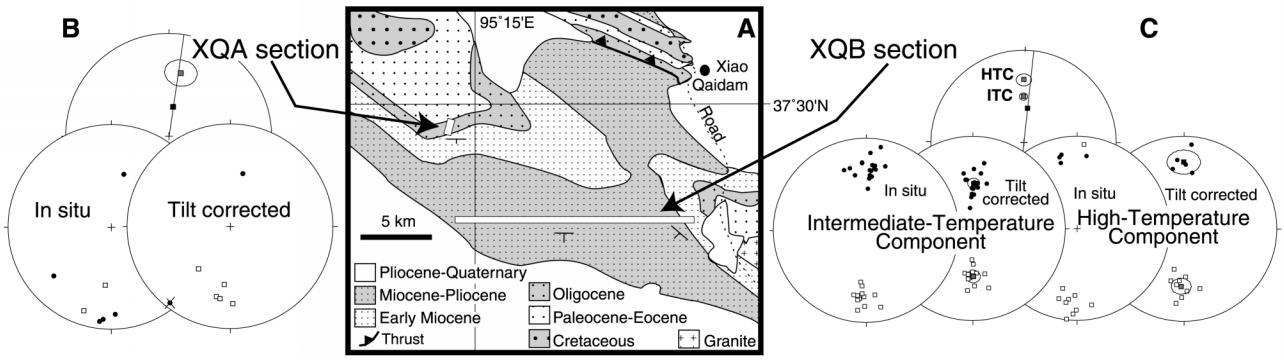

Figure 2. Paleomagnetic results from Xiao Qaidam area. A: Geologic map showing major units, structures, and locations of sampled sections. B: Equal-area projections with in situ and tilt-corrected site-mean characteristic remanent magnetization (ChRM) directions from XQA section. Filled symbols indicate directions in lower hemisphere; open symbols indicate directions in upper hemisphere; crossed symbol indicates discarded direction. Overall section-mean direction with 95% confidence limit is shown in upper projection compared with expected direction (black square) calculated from 30 Ma reference pole for Eurasia (Besse and Courtillot, 1991). Line is drawn through expected declination for comparison with observed mean declination. C: Equal-area projections of both intermediate- and high-temperature components (ITC, HTC) of ChRM from XQB section. Larger squares are mean directions for normal- and reversed-polarity groups of sites with surrounding 95% confidence limits. Overall section-mean HTC and ITC directions are compared to expected direction calculated from 10 Ma reference pole for Eurasia (Besse and Courtillot, 1991).

TABLE 1. PALAEOMAGNETIC DETERMINATIONS OF VERTICAL-AXIS ROTATION

Locality	Age (Ma)	Location		Observed Direction			Rotation $R \pm \Delta R$ (°)	Flattening $F \pm \Delta F$ (°)
		Lat (°N)	Long (°E)	I (°)	D (°)	α_{95} (°)		
Xiao Qaidam (HTC)	10	37.4	95.3	33.4	0.7	5.8	−5.6 ± 6.0	26.4 ± 4.9
Xiao Qaidam (ITC)	10	37.4	95.3	48.6	0.4	3.6	−5.9 ± 4.9	11.2 ± 3.3
Xiao Qaidam (A)	30	37.5	95.2	37.3	11.0	11.5	3.3 ± 12.0	25.6 ± 9.4
E Bo Liang	30	38.7	92.8	43.6	8.0	5.1	−0.2 ± 6.4	20.1 ± 4.4

Notes: Locality = name of paleomagnetic sampling locality. Age = age of reference Eurasian pole (Besse and Courtillot, 1991) used to calculate expected inclination and declination at the sampled locality. Location Lat = latitude of sampling locality. Location Long = longitude of sampling locality. Observed direction = mean paleomagnetic direction. I = inclination. D = declination. α_{95} = radius of 95% confidence circle. Rotation (R) = vertical-axis rotation indicated by observed declination minus expected declination (positive indicates clockwise rotation). ΔR = 95% confidence limit on rotation. Flattening (F) = flattening of inclination indicated by expected inclination minus observed inclination. ΔF = 95% confidence limit on flattening.

were determined for ITC components from 30 sites and for HTC components from 14 sites (Fig. 2C). ITC site-mean directions pass a reversal test (McFadden and McElhinny, 1990) with B classification, and HTC components pass the reversal test with C classification. A prefolding origin for both ITC and HTC components is suggested by improved clustering of site-mean directions upon restoring local bedding to horizontal compared with in situ directions (Fig. 2C), and positive fold tests (Watson and Enkin, 1993) at 99% confidence level for the HTC component and 95% for the ITC component. The important result of tectonic significance is that the mean observed declination for both the ITC and HTC components is indistinguishable from the expected declination calculated from the 10 Ma Eurasian reference pole (Besse and Courtillot, 1991) (Fig. 2B; Table 1). This result indicates that no significant vertical-axis rotation has affected the Xiao Qaidam locality since early Pliocene time. The specific limitation on clockwise rotation is that, with 95% confidence, no clockwise vertical-axis rotation exceeding 0.4° has affected this part of the Qaidam Basin since early Pliocene time.

E BO LIANG RESULTS

Situated ~30 km to the south of the Altyn Tagh fault, the E Bo Liang range (Fig. 1) is the hanging wall of an east-vergent, north-south–trending thrust fault (Fig. 3A). Paleomagnetic samples were collected from 23 sites in a 70-m-thick monoclinal section of green and reddish-brown mudstones and sandstones of the Oligocene lower Gancaigou Formation. Samples from an additional five sites were collected from an anticline at the southern end of the thrust. Thermal demagnetization of samples from 12 sites in greenish and/or coarser grained strata produced erratic behavior from which no ChRM could be determined. For samples from the remaining 16 sites, thermal demagnetization above 200 °C revealed a characteristic magnetization with unblocking temperatures dominantly <600 °C (Fig. DR1, D). From the unblocking temperatures, we interpret this stable component of magnetization to be carried predominantly by magnetite, although the presence of hematite is also indicated by rock-magnetic experiments. The resulting site-mean directions pass a reversal test (McFadden and McElhinny, 1990) with C classification. Prefolding magnetization is indicated by increase in precision parameter from 36.7 in situ to 53.7 upon restoring local bedding to horizontal and a positive fold test (Watson and Enkin, 1993) at a 95% confidence level. The section-mean declination is indistinguishable from the expected Oligocene declination (Besse and Courtillot, 1991), indicating no significant vertical-axis rotation of the E Bo Liang locality since the Oligocene (Fig. 3B; Table 1). Consistent with other paleomagnetic results along the Altyn Tagh fault (Dupont-Nivet et al., 2001), the lack of rotation of the E Bo Liang range suggests that shear associated with the left-lateral Altyn Tagh fault is localized on the fault and does not extend south into the Qaidam Basin.

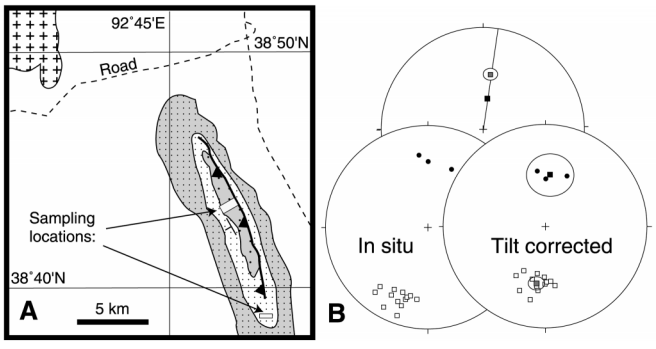

Figure 3. Paleomagnetic results from E Bo Liang locality. A: Geologic map showing major units, structures, and locations of sampled sections. B: Equal-area projections with in situ and tilt-corrected site-mean characteristic remanent magnetization directions. Symbols as in Figure 2. Overall locality-mean direction is compared with expected direction calculated from 30 Ma reference pole for Eurasia (Besse and Courtillot, 1991).

DISCUSSION AND CONCLUSIONS

An interesting feature of the paleomagnetic data from both locations is observed inclinations shallower than expected inclinations by as much as 26° (Figs. 2, B and C, and 3B; Table 1). Discordant shallow inclinations have been observed in many paleomagnetic studies of Cretaceous to Tertiary red sedimentary rocks in Asia. An important issue is whether these shallow inclinations indicate (1) northward tectonic transport (Chen et al., 1993b; Halim et al., 1998); (2) internal deformation of the Eurasian plate (Cogné et al., 1999); (3) long-lived nondipole components of the geomagnetic field (Chauvin et al., 1996; Westphal, 1993); or (4) rock-magnetic effects such as initially shallow detrital remanent magnetization or postdepositional compaction shallowing of inclination (Tan, 2001). Our results favor a rock-magnetic origin for the observed shallow inclinations from the Qaidam Basin. Interpreting the 26° shallowing of inclination for the HTC component from the XQB section by northward tectonic transport would require ~2500 km of latitudinal motion in <10 m.y., implying a velocity >25 cm/yr. In addition, deformation of the required magnitude between Siberia and Europe in the Pliocene is not evident in the geologic record. Another interesting aspect of the XQB section data set is that the inclination of the HTC carried by hematite is ~15° shallower than the inclination of the ITC carried by magnetite. Because these components recorded the same geomagnetic field, it is difficult to explain this inclination difference by external processes affecting the geomagnetic field or the reference pole. Clearly this shallow paleomagnetic direction has an internal rock-magnetic origin that we think is due to depositional effects on plate-like detrital hematite particles (Kodama, 1997; Sun and Kodama, 1992; Tauxe and Kent, 1984). We further suspect that the smaller inclination shallowing of the ITC component from the XQB section is because that component is carried by detrital magnetite, which may be less affected by shallowing of detrital remanent magnetization (Deamer and Kodama, 1990). Although the shallow paleo-

magnetic inclinations in older Cenozoic and Mesozoic red sedimentary rocks in Asia may result in part from northward tectonic transport, inaccuracies in reference paleomagnetic poles, and nondipole components of the geomagnetic field, our observations clearly indicate that rock-magnetic effects dominate in some geologic units.

Mean paleomagnetic declinations from two locations separated by several hundred kilometers within the Qaidam Basin indicate no vertical-axis rotation during the past 30 m.y. Kinematic models (Peltzer and Saucier, 1996) implying clockwise rotation of the Qaidam Basin at rates approaching 1°/m.y. cannot be extrapolated to Oligocene time. Because the Altyn Tagh fault forms the northern boundary of the Qaidam Basin, our results indicate no Neogene rotation of this lithospheric-scale fault (Wittlinger et al., 1998). In contrast, paleomagnetic results from areas east of the Qaidam Basin and north of the Kunlun fault (Frost et al., 1995; Halim et al., 1998; Cogné et al., 1999) indicate clockwise vertical-axis rotations of 15°–30° (Fig. 1; Table DR2 [see footnote 1]). The Qaidam Basin may act as an indentor translating without rotation toward the North China block and driving clockwise vertical-axis rotations by differential shortening within the Nan Shan fold-and-thrust belt. South of the Kunlun fault, oroclinal bending north of the eastern Himalayan syntaxis is suggested by curved strike-slip faults and paleomagnetic data indicating increasing amounts of clockwise rotation toward the southeast within the Qiangtang terrane (Fig. 1; Table DR2 [see footnote 1]). This pattern of rotations is consistent with right-slip simple shear of the eastern Tibetan Plateau (England and Molnar, 1990). The change in geodynamics across the Kunlun fault may result from viscous flow of lower crust and mantle lithosphere south of the fault (Owens and Zandt, 1997; Royden et al., 1997), in contrast to stronger lower crust and mantle lithosphere within the Kunlun-Qaidam terrane north of the Kunlun fault (Zhu and Helmberger, 1998).

ACKNOWLEDGMENTS

This research was funded by the Continental Dynamics Program of the National Science Foundation. Logistical support was provided by Wang Xiao Feng and the Institute of Geomechanics, Beijing, People's Republic of China. Laboratory assistance was provided by Bill Hart and Lucas Murray. Discussions with George Zandt and George Gehrels improved the manuscript. We also thank an anonymous reader, Vincent Courtillot, and Ben van der Pluijm for careful reviews of this manuscript.

REFERENCES CITED

Beck, M.E., Burmester, R.F., Craig, D.E., Grommé, C.S., and Wells, R.E., 1986, Paleomagnetism of middle Tertiary volcanic rocks from the Western Cascade series, northern California: Timing and scale of rotation in the southern Cascades and Clamath mountains: Journal of Geophysical Research, v. 91, p. 8219–8230.

Bendick, R., Bilham, R., Freymueller, J., Larson, K., and Yin, G., 2000, Geodetic evidence for a low slip rate in the Altyn Tagh fault system: Nature, v. 404, p. 69–72.

Besse, J., and Courtillot, V., 1991, Revised and synthetic apparent polar wander paths of the African, Eurasian, North American and Indian plates, and true polar wander since 200 Ma: Journal of Geophysical Research, v. 96, p. 4029–4050.

Chauvin, A., Perroud, H., and Bazhenov, M.L., 1996, Anomalous low palaeomagnetic inclinations from Oligocene–Lower Miocene red beds of the south-west Tien Shan, Central Asia: Geophysical Journal International, v. 126, p. 303–313.

Chen, Y., Cogne, J.-P., Courtillot, V., Tapponnier, P., and Zhou, X.Y., 1993a, Cretaceous paleomagnetic results from western Tibet and tectonic implications: Journal of Geophysical Research, v. 98, p. 17 981–18 000.

Chen, Y., Courtillot, V., Cogne, J.-P., Besse, J., Yang, Z., and Enkin, R., 1993b, The configuration of Asia prior to the collision of India: Cretaceous paleomagnetic constraints: Journal of Geophysical Research, v. 98, p. 21 927–21 941.

Chen, Z., Burchfiel, B.C., Liu, Y., King, R.W., Royden, L.H., Tang, W., Wang, E., Zhao, J., and Zhang, X., 2000, Global Positioning System measurements from eastern Tibet and their implications for India/Eurasia intercontinental deformation: Journal of Geophysical Research, v. 105, p. 16 215–16 227.

Cogné, J.P., Halim, N., Chen, Y., and Courtillot, V., 1999, Resolving the problem of shallow magnetizations of Tertiary age in Asia: Insights from paleomagnetic data from the Qiangtang, Kunlun, and Qaidam blocks (Tibet, China), and a new hypothesis: Journal of Geophysical Research, v. 104, p. 17 715–17 734.

Deamer, G.A., and Kodama, K.P., 1990, Compaction-induced inclination shallowing in synthetic and natural clay-rich sediments: Journal of Geophysical Research, v. 95, p. 4511–4529.

Dupont-Nivet, G., Butler, R.F., Yin, A., Robinson, D., Zhang, Y., and Qiao, W.S., 2001, Paleomagnetism on arcuate structures along the Altyn Tagh fault: implications for the intracontinental deformation processes in Asia [abstract T12F-06]: Eos (Transactions, American Geophysical Union), v. 82, p. F1125.

England, P., and Houseman, G., 1986, Finite strain calculation of continental deformation, 2, Comparison with the India-Asia collision zone: Journal of Geophysical Research, v. 91, p. 3664–3676.

England, P., and Molnar, P., 1990, Right-lateral shear and rotation as the explanation for strike-slip faulting in eastern Tibet: Nature, v. 344, p. 140–142.

Fisher, R.A., 1953, Dispersion on a sphere: Royal Society London Proceedings, v. 217A, p. 295–305.

Frost, G.M., Coe, R.S., Meng, Z., Peng, Z., Chen, Y., Courtillot, V., Peltzer, G., Tapponnier, P., and Avouac, J.P., 1995, Preliminary Early Cretaceous paleomagnetic results from the Gansu Corridor, China: Earth and Planetary Science Letters, v. 129, p. 217–232.

Gilder, S., Zhao, X., Coe, R., Meng, Z., Courtillot, V., and Besse, J., 1996, Paleomagnetism and tectonics of the southern Tarim Basin, northwestern China: Journal of Geophysical Research, v. 101, p. 22 015–22 031.

Halim, N., Cogné, J.P., Chen, Y., Atasiesi, R., Besse, J., Courtillot, V., Gilder, S., Marcoux, J., and Zhao, R.L., 1998, New Cretaceous and early Tertiary paleomagnetic results from Xining-Lanzhou basin, Kunlun and Qiangtang blocks, China: Implications on the geodynamic evolution of Asia: Journal of Geophysical Research, v. 103, p. 21 025–21 045.

Holt, W.E., and Haines, A.J., 1993, Velocity fields in deforming Asia from the inversion of earthquake-released strains: Tectonics, v. 12, p. 1–20.

Kirschvink, J.L., 1980, The least-square line and plane and the analysis of paleomagnetic data: Royal Astronomical Society Geophysical Journal, v. 62, p. 699–718.

Kodama, K.P., 1997, A successful rock magnetic technique for correcting paleomagnetic inclination shallowing: Case study of the Nacimiento Formation, New Mexico: Journal of Geophysical Research, v. 102, p. 5193–5205.

McFadden, P.L., 1990, A new fold test for paleomagnetic studies: Geophysical Journal International, v. 103, p. 163–169.

McFadden, P.L., and McElhinny, M.W., 1990, Classification of the reversal test in palaeomagnetism: Geophysical Journal International, v. 103, p. 725–729.

Meyer, B., Tapponnier, P., Bourjot, L., Metivier, F., Gaudemer, Y., Peltzer, G., Shummin, G., and Chen, Z., 1998, Crustal thickening in the Gansu-Qinghai, lithospheric mantle, oblique and strike-slip controlled growth of the Tibetan Plateau: Geophysical Journal International, v. 135, p. 1–47.

Owens, T.J., and Zandt, G., 1997, Implication of crustal property variations for models of the Tibetan plateau evolution: Nature, v. 387, p. 37–43.

Peltzer, G., and Saucier, F., 1996, Present-day kinematics of Asia derived from geologic fault rates: Journal of Geophysical Research, v. 101, p. 27 943–27 956.

Qinghai Bureau of Geology and Mineral Resources, 1991, Regional geology of the Qinghai Province: Beijing, Geological Publishing House, 662 p.

Royden, L.H., Burchfiel, B.C., King, R.W., Wang, E.W., Chen, Z., Shen, F., and Liu, Y., 1997, Surface deformation and lower crustal flow in eastern Tibet: Science, v. 276, p. 788–790.

Sun, W.W., and Kodama, K.P., 1992, Magnetic anisotropy, scanning electron microscopy, and X-ray pole figure goniometry study of inclination shallowing in a compacting clay-rich sediment: Journal of Geophysical Research, v. 97, p. 19 599–19 615.

Tan, X., 2001, Correcting the bias toward shallow paleomagnetic inclinations in hematite-bearing sedimentary rocks: Theory, experiments, and applications [Ph.D. thesis]: Bethlehem, Pennsylvania, Lehigh University.

Tapponnier, P., Peltzer, G., Le Dain, A.Y., and Armijo, R., 1982, Propagating extrusion tectonics in Asia: New insights from simple experiments with Plasticine: Geology, v. 10, p. 611–616.

Tauxe, L., and Kent, D.V., 1984, Properties of a detrital remanence carried by haematite from study of modern river deposits and laboratory redeposition experiments: Royal Astronomical Society Geophysical Journal, v. 77, p. 543–561.

Watson, G.S., and Enkin, R.J., 1993, The fold test in paleomagnetism as a parameter estimation problem: Geophysical Research Letters, v. 20, p. 2135–2137.

Westphal, M., 1993, Did a large departure from the geocentric axial dipole hypothesis occur during the Eocene? Evidence from the magnetic polar wander path of Eurasia: Earth and Planetary Science Letters, v. 117, p. 15–28.

Wittlinger, G., Tapponnier, P., Poupinet, G., Mei, J., Danian, S., Herquel, G., and Masson, F., 1998, Tomographic evidence for localized lithospheric shear along the Altyn Tagh fault: Science, v. 282, p. 74–76.

Yin, A., and Harrison, T.M., 2000, Geologic evolution of the Himalayan-Tibetan orogen: Annual Reviews of Earth and Planetary Science, v. 28, p. 211–280.

Zhu, L., and Helmberger, D.V., 1998, Moho offset across the northern margin of the Tibetan Plateau: Science, v. 281, p. 1170–1172.

Zhu, L., Owens, T.J., and Randall, G.E., 1995, Lateral variation in crustal structure of the northern Tibetan Plateau inferred from teleseismic receiver functions: Seismological Society of America Bulletin, v. 85, p. 1531–1540.

Manuscript received August 8, 2001
Revised manuscript received November 16, 2001
Manuscript accepted November 20, 2001

Printed in USA

Data Repository item

TABLE DR1. SITE-MEAN PALEOMAGNETIC DIRECTIONS

	Geographic		Stratigraphic						
Site No.	*I* (°)	*D* (°)	*I* (°)	*D* (°)	α_{95} (°)	*k*	*N*	Dip az. (°)	Dip (°)
E BO LIANG SECTION									
GN004	-26.4	218.4	-50.0	205.9	11.8	23.2	7	246	28
GN006	-25.2	208.1	-45.3	193.8	4.4	165.3	7	246	28
GN007	-19.0	218.9	-43.0	210.0	7.5	68.0	6	246	28
GN010	-11.2	208.8	-32.5	201.3	5.4	91.7	8	246	28
GN012	-19.5	198.5	-36.4	186.2	20.3	12.1	5	246	28
GN013	-27.1	197.1	-42.6	180.3	5.9	135.7	5	246	28
GN014	-31.5	207.9	-51.0	189.5	6.8	59.4	8	246	28
GN015	-29.2	196.6	-44.2	178.4	9.6	35.0	7	246	28
GN016	-32.2	201.1	-48.8	181.1	6.1	72.2	8	246	28
GN017	-22.4	201.9	-40.4	188.4	5.1	179.6	5	246	28
GN018	-9.4	198.9	-27.4	191.5	9.2	32.5	8	246	28
GN021	29.4	353.4	44.4	352.2	10.5	34.7	6	179	15
GN022	35.4	0.7	51.4	1.2	4.7	173.1	6	179	16
GN023	38.5	22.8	45.5	23.7	3.7	223.3	7	195	7
GN024	-29.1	188.5	-40.6	170.2	11.2	38.0	5	246	28
GN026	-31.1	193.7	-44.6	174.0	8.2	46.8	7	246	28
AVG.	26.5	20.0			6.2	36.7	16	Geographic	
AVG.			43.6	8.0	5.1	53.7	16	Stratigraphic	
XQA SECTION									
XQ039	-42.5	185.7	-42.5	185.7	11.0	31.3	7	0	0
XQ043	45.9	13.7	45.9	13.7	19.9	15.7	5	0	0
XQ051	-22.9	201.0	-46.9	216.4	10.9	32.5	6	163.5	42
XQ052	7.8	186.8	-30.8	190.7	8.9	39.6	8	163.5	42
XQ053	15.9	177.0	-25.3	177.9	12.3	24.9	7	163.5	42
XQ054	10.2	184.9	-29.0	187.8	14.5	15.5	8	163.5	42
XQ055*	27.4	229.1	5.3	217.8	7.8	51.5	8	163.5	42
AVG.	12.8	7.9			25.1	8.1	6	Geographic	
AVG.			37.3	11.0	11.5	34.8	6	Stratigraphic	
XQB SECTION High Temperature Component									
XQ002	-12.0	180.3	-33.0	176.9	12.3	21.2	8	200	23
XQ003	21.4	346.2	31.1	1.8	13.5	17.9	8	101	32
XQ004	19.8	348.1	26.3	354.8	10.2	30.2	8	104	17
XQ005	27.9	346.4	34.7	349.8	10.1	31.2	8	135	8
XQ007	-27.6	181.4	-46.5	177.7	11.2	30.2	7	194	20
XQ008	-22.4	194.2	-41.9	194.2	17.0	21.2	5	194	20
XQ009	19.4	9.2	38.8	8.2	6.5	87.4	7	194	20
XQ010	-20.6	180.7	-39.5	177.7	8.5	42.9	8	194	20
XQ012	-16.3	169.2	-33.8	165.1	7.4	68.0	7	194	20
XQ013	-23.7	186.7	-43.0	184.8	12.7	23.5	7	194	20
XQ014	-1.1	186.5	-20.4	186.0	6.6	70.5	8	194	20
XQ018	-19.4	188.2	-38.8	187.0	9.1	54.8	6	194	20

XQ028	-9.7	5.0	9.5	5.0	21.4	19.4	4	194	20
XQ033	-7.6	182.7	-26.6	181.5	14.4	29.1	5	194	20
AVG.	16.6	0.4			6.8	35.6	14	Geographic	
AVG.			33.4	0.7	5.8	47.9	14	Stratigraphic	

XQB SECTION Intermediate Temperature Component

XQ002	-28.6	181.7	-49.5	174.8	6.3	77.3	8	200	23
XQ003	31.4	345.6	39.4	8.5	15.2	20.3	6	101	32
XQ004	30.9	340.0	39.2	350.6	5.5	103.7	8	104	17
XQ005	39.3	348.7	45.8	353.0	5.6	97.2	8	135	8
XQ006	52.8	2.9	71.7	352.4	9.0	39.0	8	194	20
XQ007	-31.6	183.6	-50.7	180.0	6.6	72.2	8	194	20
XQ008	-29.5	190.9	-48.9	189.9	8.7	48.6	7	194	20
XQ009	32.5	7.8	51.8	5.6	7.1	61.9	8	194	20
XQ010	-26.2	185.2	-45.4	182.7	6.9	64.5	8	194	20
XQ011	-42.9	185.7	-62.1	180.9	12.4	30.1	6	194	20
XQ012	-30.2	172.0	-47.9	165.1	9.1	45.2	7	194	20
XQ013	-29.4	187.4	-48.7	185.2	7.6	54.5	8	194	20
XQ014	-13.8	185.9	-33.0	184.6	5.6	119.2	7	194	20
XQ017	-16.0	169.3	-33.5	165.2	24.2	11.0	5	194	20
XQ018	-24.8	186.8	-44.1	184.9	6.4	89.9	7	194	20
XQ019	35.0	3.4	54.1	359.1	6.3	91.6	7	194	20
XQ020	39.9	4.2	59.0	359.4	10.7	27.7	8	194	20
XQ021	29.4	5.5	48.6	2.8	3.7	269.8	7	194	20
XQ022	9.2	10.2	28.6	9.7	7.3	68.5	7	194	20
XQ023	33.9	8.9	53.2	6.9	3.5	258.1	8	194	20
XQ024	29.6	7.8	49.0	5.7	7.7	53.2	8	194	20
XQ025	27.6	356.9	46.0	352.0	7.6	78.2	6	194	20
XQ026	-39.1	184.1	-58.2	179.3	10.5	28.8	8	194	20
XQ027	28.4	16.9	47.9	17.8	6.1	82.3	8	194	20
XQ028	16.7	3.5	35.9	1.5	5.8	91.0	8	194	20
XQ029	40.8	6.0	60.0	1.8	4.3	245.8	6	194	20
XQ030	35.5	4.9	54.6	1.1	10.4	34.8	7	194	20
XQ031	27.4	356.8	45.8	351.9	6.1	84.6	8	194	20
XQ032	43.0	3.3	62.0	357.2	5.2	98.2	9	194	20
XQ033	-18.7	180.8	-37.6	178.2	7.3	58.8	8	194	20
AVG.	30.7	2.2			3.8	48.3	30	Geographic	
AVG.			48.6	0.4	3.6	55.6	30	Stratigraphic	

Notes: Site No. - number for paleomagnetic site; *I* and *D* - inclination and declination of site-mean direction in geographic coordinates (with no structural correction) and stratigraphic coordinates (after restoration of local bedding to horizontal); α_{95} - radius of cone of 95% confidence about site-mean direction; *k* - concentration parameter; *N* - number of samples averaged to calculate site-mean paleomagnetic direction; Dip Az. - azimuth of down dip direction of local bedding; Dip - angle of dip of local bedding; AVG. - average direction for sampled section calculated by treating each site-mean direction as a unit vector is given in stratigraphic and geographic coordinates; * - discarded site.

Data Repository item

TABLE DR2. PALAEOMAGNETIC RESULTS OF THE EASTERN TIBETAN PLATEAU

Direction-space analysis									
Locality	Age	Location		Observed Direction			Rotation	Flattening	Reference
		Lat	Long	I	D	α_{95}	$R \pm \Delta R$	$F \pm \Delta F$	
	(Ma)	(°N)	(°E)	(°)	(°)	(°)	(°)	(°)	
Xiao Qaidam (HTC)	10	37.4	95.3	33.4	0.7	5.8	-5.6 ± 6.0	26.4 ± 4.9	This study
Xiao Qaidam (ITC)	10	37.4	95.3	48.6	0.4	3.6	-5.9 ± 4.9	11.2 ± 3.3	This study
Xiao Qaidam (A)	30	37.5	95.2	37.3	11.0	11.5	3.3 ± 12.0	25.6 ± 9.4	This study
E Bo Liang	30	38.7	92.8	43.6	8.0	5.1	-0.2 ± 6.4	20.1 ± 4.4	This study
Yushu	10	33.2	96.7	30.7	35.6	9.0	29.8 ± 8.7	25.4 ± 7.4	1
Tuoluo Lake	20	35.3	98.6	46.2	20.1	27.1	12.5 ± 33.1	13.1 ± 21.8	1
Jungong	10	34.7	100.7	33.5	19.8	6.0	14.2 ± 6.2	24.3 ± 5.1	1
Xining	40	36.5	102.0	40.8	29.3	13.2	20.1 ± 14.6	21.2 ± 10.8	1
Xining-Lanzhou	120	36.2	103.5	44.1	44.7	5.1	27.8 ± 6.8	5.5 ± 5.5	2
Fenghuoshan	50	34.5	92.8	34.6	25.5	6.0	12.3 ± 7.4	25.1 ± 5.7	2, 3
Hekou group	120	39.0	99.6	39.0	41.9	5.1	25.1 ± 6.5	12.6 ± 5.4	4
Pole-space analysis									
Locality	Age	Location		Observed Pole			Rotation	Translation	Reference
		Lat	Long	Lat	Long	A_{95}	$R \pm \Delta R$	$p \pm \Delta p$	
	(Ma)	(°N)	(°E)	(°N)	(°E)	(°)	(°)	(°)	
Mangkang	80	29.7	98.6	48.6	173.5	6.0	33.6 ± 7.2	-4.5 ± 6.2	5, 6
South China block	80	30.0	102.9	72.8	241.1	5.0	3.7 ± 5.2	11.0 ± 4.8	7
South China block	80	26.5	102.4	81.5	220.9	7.1	7.0 ± 6.8	1.9 ± 6.3	5
South China block	120	27.9	102.3	77.4	196.2	14.0	3.5 ± 13.3	-3.6 ± 11.9	8
South China block	120	26.8	102.5	69.0	204.6	4.3	4.5 ± 5.7	1.0 ± 5.3	5

Notes: Locality = name of paleomagnetic sampling locality. Age = age of reference Eurasian pole (Besse and Courtillot, 1991) used to calculate expected inclination and declination at the sampled locality. Location Lat = latitude of sampling locality. Location Long = longitude of sampling locality. Observed direction = mean paleomagnetic direction. I = inclination. D = declination. α_{95} = radius of 95% confidence circle. Rotation (R) = vertical-axis rotation indicated by observed declination minus expected declination (positive indicates clockwise rotation). ΔR = 95% confidence limit on rotation. Flattening (F) = flattening of inclination indicated by expected inclination minus observed inclination. ΔF = 95% confidence limit on flattening. Observed pole = observed paleomagnetic pole at sampling locality. A_{95} = 95% confidence limit on observed pole. Translation (p) = distance of sampling locality from observed pole minus distance from reference pole; Δp = 95% confidence limit on translation. References: 1, Cogné et al. (1999); 2, Halim et al. (1998); 3, Lin and Watts (1988); 4, Frost et al. (1995); 5, Huang et al. (1992); 6, Otofuji et al. (1990); 7, Enkin et al. (1991); 8, Zhu et al. (1988).

Besse, J., and Courtillot, V., 1991, Revised and synthetic apparent polar wander paths of the African, Eurasian, North American and Indian plates, and true polar wander since 200 Ma: Journal of Geophysical Research, v. 96, p. 4029-4050.

Cogné, J.P., Halim, N., Chen, Y., and Courtillot, V., 1999, Resolving the problem of shallow magnetizations of Tertiary age in Asia: Insights from paleomagnetic data from the Qiangtang, Kunlun, and Qaidam blocks (Tibet, China), and a new hypothesis: Journal of Geophysical research, v. 104, p. 17715-17734.

Enkin, R.J., Chen, Y., Courtillot, V., Besse, J., Xing, L., Zhang, Z., Zhuang, Z., and Zhang, J., 1991, A Cretaceous pole from south China, and the Mesozoic hairpin turn of the Eurasian apparent polar wander path: Journal of Geophysical Research, v. 96, p. 4007-4027.

Frost, G.M., Coe, R.S., Meng, Z., Peng, Z., Chen, Y., Courtillot, V., Peltzer, G., Tapponnier, P., and Avouac, J.P., 1995, Preliminary early Cretaceous paleomagnetic results from the Gansu Corridor, China: Earth and Planetary Science Letters, v. 129, p. 217-232.

Halim, N., Cogné, J.P., Chen, Y., Atasiesi, R., Besse, J., Courtillot, V., Gilder, S., Marcoux, J., and Zhao, R.L., 1998, New Cretaceous and early Tertiary paleomagnetic results from Xining-Lanzhou basin, Kunlun and Qiangtang blocks, China: Implications on the geodynamic evolution of Asia.: Journal of Geophysical Research, v. 103, p. 21025-21045.

Huang, K., Opdyke, N.D., Li, J., and Peng, X., 1992, Paleomagnetism of Cretaceous rocks from eastern Qiangtang terrane of Tibet: Journal of Geophysical Research, v. 97, p. 1789-1799.

Lin, J., and Watts, D.R., 1988, Paleomagnetic results from the Tibetan plateau: Royal Society of London Philosophical Transactions, v. 327, p. 239-262.

Otofuji, Y., Inoue, S., Funahara, S., Murata, F., and Zheng, X., 1990, Palaeomagnetic study of eastern Tibet-Deformation of the Three Rivers region: Geophysics Journal International, v. 103, p. 85-94.

Zhu, Z.W., Hao, T., and Zhao, H., 1988, Paleomagnetic study on the tectonic motion of Pan-Xi block and adjacent area during Yin Zhi - Yanshan period: Acta Geophysica Sinica, v. 31, p. 420-431.

DATA REPOSITORY ITEM

Dupont-Nivet et al. Figure DR1

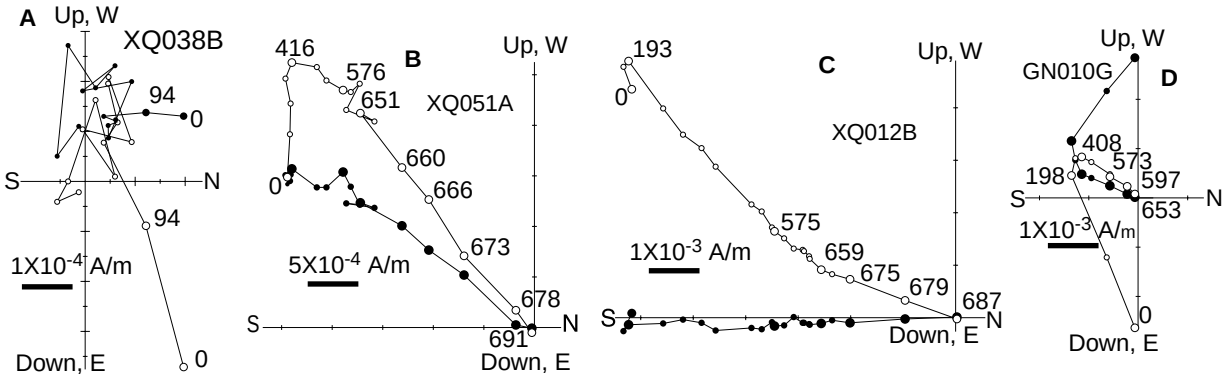

Figure DR1. Vector-component diagrams of thermal-demagnetization behavior. A: Sample XQ038B from Xiao Qaidam area from which characteristic remanent magnetization direction could not be determined. B: Sample XQ051A from XQA section, Xiao Qaidam area. C: Sample XQ012B from XQB section, Xiao Qaidam area. D: Sample GN010G from E Bo Liang range. Open circles are projections onto vertical plane, and filled circles are projections onto horizontal plane. Numbers adjacent to data points indicate temperature (in °C).